BNWL-1522-4
UC-80

Battelle
Pacific Northwest Laboratories
Richland, Washington 99352

AEC Research and Development Report

TECHNICAL ACTIVITIES
QUARTERLY REPORT

AEC REACTOR DEVELOPMENT
AND TECHNOLOGY PROGRAMS

JULY, AUGUST, SEPTEMBER 1971

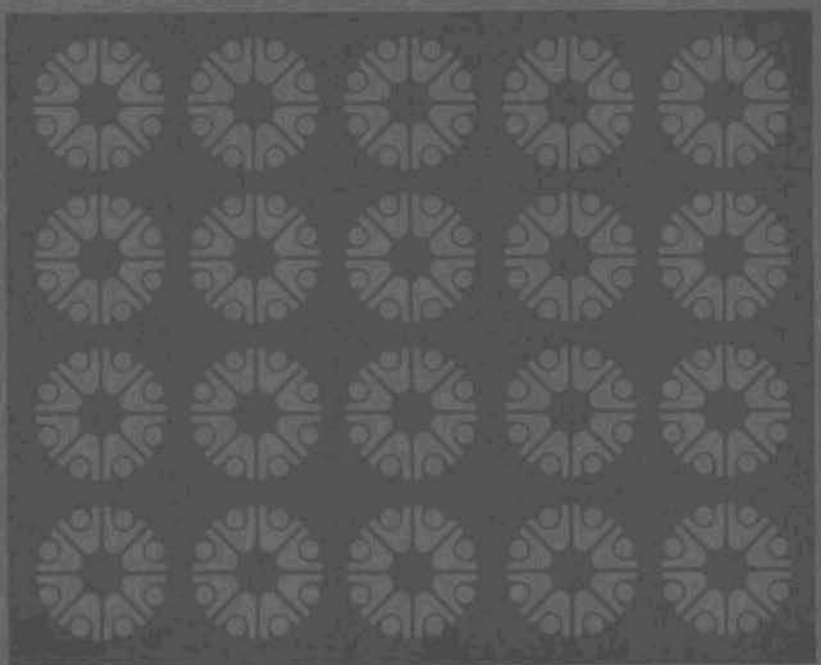

BNWL-1522-4

NOTICE

This report was prepared as an account of work sponsored by the United States Government. Neither the United States nor the United States Atomic Energy Commission, nor any of their employees, makes any warranty, express or implied, or assumes any legal liability or responsibility for the accuracy, completeness or usefulness of any information, apparatus, product, or process disclosed, or represents that its use would not infringe privately-owned rights.

PACIFIC NORTHWEST LABORATORY
operated by
BATTELLE
for the
U.S. ATOMIC ENERGY COMMISSION
Under Contract AT(45-1)-1830

Printed in the United States of America
Available from
National Technical Information Service
U.S. Department of Commerce
5285 Port Royal Road
Springfield, Virginia 22151
Price: Printed Copy $3.00; Microfiche $0.95

AEC-RL RICHLAND, WASH

3 3679 00061 7805

BNWL-1522-4

UC-80,
Reactor Technology

TECHNICAL ACTIVITIES QUARTERLY REPORT
AEC REACTOR DEVELOPMENT
AND TECHNOLOGY PROGRAMS
JULY, AUGUST, SEPTEMBER 1971

By

Staff of Battelle-Northwest

Program Cordinator:
L. C. Schmid

December 1971

BATTELLE
PACIFIC NORTHWEST LABORATORIES
RICHLAND, WASHINGTON 99352

TECHNICAL ACTIVITIES QUARTERLY REPORT
AEC REACTOR DEVELOPMENT
AND TECHNOLOGY PROGRAMS
JULY, AUGUST, SEPTEMBER 1971

FOREWORD

This report covers all programs except the Waste Studies Program conducted at the Pacific Northwest Laboratory for the U.S. Atomic Energy Commission's Reactor Development and Technology Division. The objective of the Technical Activities Quarterly Report is to inform the scientific community in a timely manner of the technical progress made on the programs. The report contains brief technical discussions of accomplishments in all areas where significant progress has been made during the reporting period. The results presented should be considered preliminary and do not constitute final publication of the work. A list of publications and papers is given in the report. Anyone wishing to obtain additional information on the work presented is encouraged to contact the author directly.

CONTENTS

1. SUMMARY

HIGH TEMPERATURE REACTOR PHYSICS

The analysis of the Molten Salt Breeder Reactor lattice experiment in the HTLTR has been completed. The temperature coefficient was found to be smaller than the calculated value at all temperatures.

Experiments in the HTLTR with a ThO_2-PuO_2 HTGR lattice have been successfully concluded. Relative reactivity worths of fuel and poison blocks were measured as a function of temperature up to 1000°C. The effect of neutron upscatter into the low-lying resonances of plutonium on the temperature-dependent reactivity behavior is increasingly important at elevated temperatures.

STEADY STATE AND TRANSIENT SUBCHANNEL CODE DEVELOPMENT AND DATA ANALYSIS

The major effort of this reporting period was the further development of an improved transverse momentum and forced crossflow mixing model for the COBRA-III computer program. A new transverse momentum equation was derived and now includes the temporal and axial component of spatial acceleration. The axial momentum equation was simplified by assuming the axial velocity of the crossflow to be equal to the velocity of the subchannel. This simplification is justified and significantly improves computation speed. A wire wrap forced mixing model has been incorporated into the COBRA-III program.

EFFECT OF ^{241}Pu ON CRITICALITY SAFETY LIMITS FOR ^{239}Pu

Criticality experiments were carried out with a plutonium nitrate solution containing 42.9 wt% ^{240}Pu and 10.9 wt% ^{241}Pu. Plutonium concentrations were varied from 40 to 140 g/ℓ and acid molarity varied from 1.5 to 5M. A stainless steel cylindrical vessel was used. Data obtained from these experiments are presented.

NUCLEAR GRAPHITE

Compressive creep capsules operating at 550 and 800°C and a tensile creep capsule operating at 800°C were charged into the ETR in September. The first two are scheduled for a three-cycle irradiation and the latter for a one-cycle irradiation.

The gas phase radiolysis study of helium diluted equimolar mixtures of CO and H_2O has been extended to 100, 240, and 465 vpm. The data were fit to equations of the form G (molecules/100 eV) = $aT^{1/2}\ e^{-E/RT}$. The constants (a) and activation energies (E) are shown to vary as a function of reactant concentration.

The cold-seeding capsule was ready for shipment to Idaho Falls to begin the third high-temperature irradiation period starting in November.

The high-temperature graphite-irradiation capsule, GEH-13-422, was inserted in the ETR at the beginning of Cycle 113.

A report (BNWL-SA-3985) on irradiation-induced changes in glassy carbons, has been issued and submitted to Carbon. The results reported therein appear to resolve a previously reported anomaly in regard to the effect of irradiation on crystallite perfection.

PHOENIX FUEL STUDIES

Fuel burnup information has been obtained from nondestructive and destructive examinations of fuel plates and flux monitor wands removed from the MTR-Phoenix fuel core. The isotopic data have been used in a multivariable least squares analysis to derive ratios of effective cross sections for the fuel isotopes. Marked differences were noted in the effective cross sections for fuel located in the core interior and in the core boundary regions.

2. HIGH TEMPERATURE REACTOR PHYSICS

MEASUREMENT OF PHYSICS PARAMETERS FOR AN MSBR LATTICE IN THE HTLTR

E. P. Lippincott

Analysis of measurements made on the Molten Salt Breeder Reactor (MSBR) lattice in the HTLTR has been completed. A detailed description of the results is being prepared and will be presented as a document with the above title.

The basic lattice and preliminary results have been described in previous quarterly reports.[1,2] The experimental value of k_∞ at each temperature is presented in Table 2.1 and is compared to values calculated using EGGNIT[3] for the neutron energy region above 0.683 eV and GRANIT[4] for the thermal region. The experimental k_∞ lies below the calculation at all temperatures, and the change with temperature is much smaller than predicted. The result for the change of k_∞ with temperature is in qualitative agreement with two previous ThO_2-$^{233}UO_2$ lattices in the HTGR series in the HTLTR.[5,6]

TABLE 2.1. Infinite Medium Multiplication Factors

Temperature, °C	Experimental k_∞	Calculated k_∞
20	1.0291 ± 0.0012	1.0479
300	1.0127 ± 0.0010	1.0269
627	1.0065 ± 0.0010	1.0136
1000	1.0037 ± 0.0012	1.0051

In addition to the evaluation of k_∞ for the basic lattice cell, an evaluation was made including the graphite end cap region. To calculate k_∞ for comparison, the end cap graphite was smeared into the cell moderator. The result obtained for the temperature coefficient was little affected by this treatment.

References

1. *E. C. Davis and E. P. Lippincott, "Design of MSBR Experiment in the HTLTR," Technical Activities Quarterly Report, AEC Reactor Development and Technology Programs, October 1970-March 1971, BNWL-1522-2, Battelle-Northwest, June 1971.*

2. *E. P. Lippincott, "Reactivity Measurements in a Mockup MSBR Lattice in the HTLTR," Technical Activities Quarterly Report, AEC Reactor Development and Technology Programs, April, May, June 1971, BNWL-1522-3, Battelle-Northwest, October 1971.*

3. *C. R. Rickey, EGGNIT: A Multigroup Cross Section Code, BNWL-1203, Battelle-Northwest, November 1969.*

4. *C. L. Bennett, "GRANIT: A Code for Calculating Position Dependent Thermal Neutron Spectra in Doubly Heterogeneous Systems by the Integral Transport Method," Technical Activities Quarterly Report, AEC Reactor Development and Technology Programs, July, August, September 1970, BNWL-1522-1, p. 2.48, Battelle-Northwest, October 1970.*

5. *E. P. Lippincott, Measurement of the Temperature Dependence of k_∞ for a $^{233}UO_2$-ThO_2 HTGR Lattice, BNWL-1561, Battelle-Northwest, May 1971.*

6. *T. J. Oakes, Measurement of k_∞ as a Function of Temperature for a $^{233}UO_2$-$^{232}ThO_2$-C Lattice, BNWL-1601, Battelle-Northwest, 1971.*

REACTIVITY MEASUREMENTS FOR A ThO_2-PuO_2 HTGR LATTICE IN THE HTLTR AS A FUNCTION OF TEMPERATURE

D. F. Newman

Experiments in the HTLTR using a High Temperature Gas-Cooled Reactor (HTGR) lattice fueled with a ThO_2-PuO_2 fuel blend[1] were successfully concluded during September. Measurements of relative reactivity worths of the ThO_2-PuO_2 central cell, the V_2O_3-PuO_2 central cell, and the normalizing copper absorber were completed with the reactor in thermal equilibrium at temperatures of 20, 300, 500, 750, and 1000°C. In addition, the reactivity worths of single $^{235}UC_2$ and $^{233}UO_2$ fueled HTGR blocks, poison blocks, and graphite were measured at each temperature.

In general, the relative reactivity worths of fuel and poison blocks were quite different than in previous HTGR lattices.[2,3] Comparison (Figure 2.1) of relative reactivity worths of the ThO_2-PuO_2 central cell

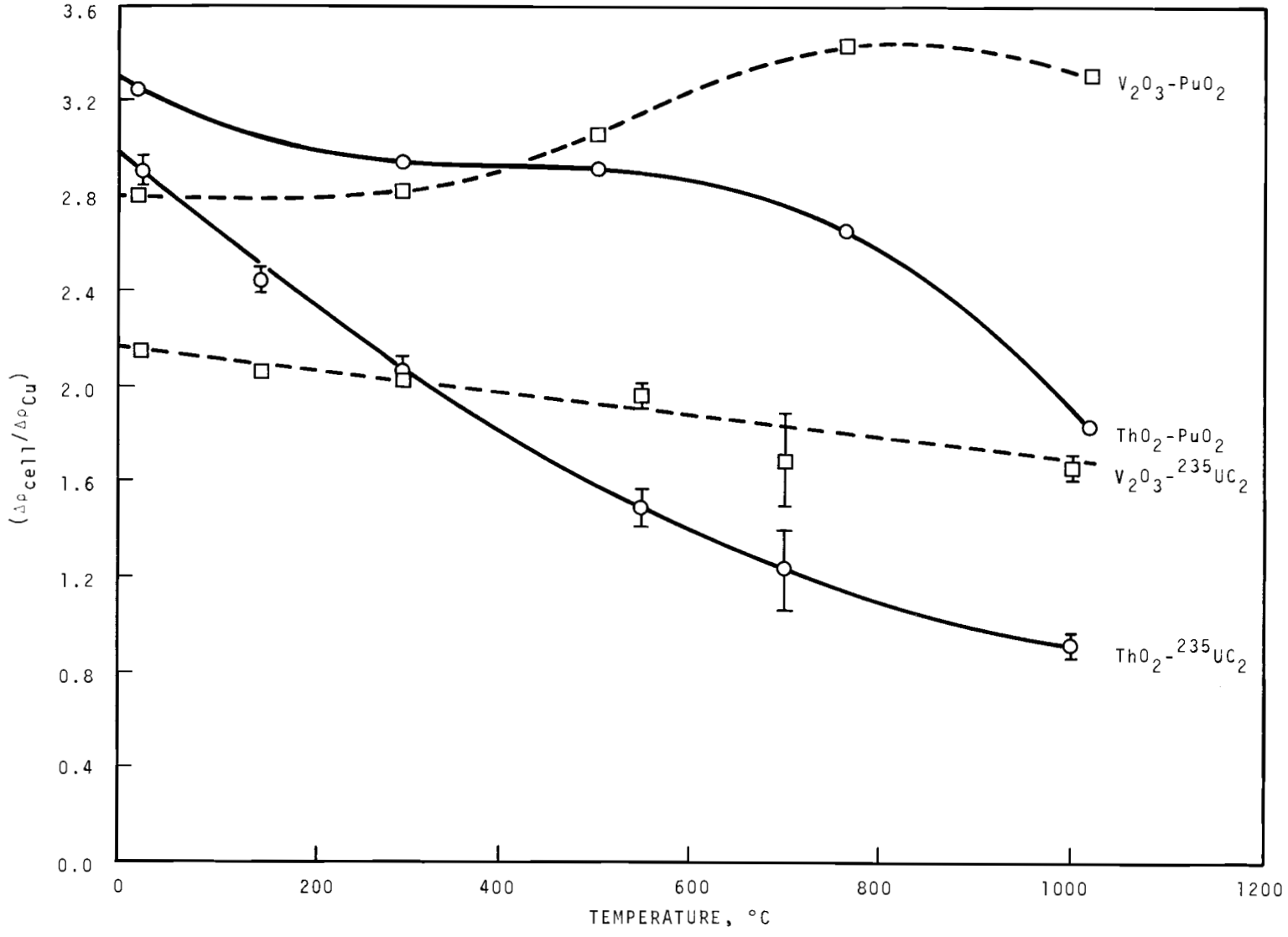

FIGURE 2.1. Reactivity Worth (Normalized to Copper) as a Function of Temperature

and the V_2O_3-PuO_2 central cell normalized to copper with similar measurements in the ThO_2-$^{235}UC_2$ HTGR lattice shows the effect of the low-lying resonances of ^{239}Pu and ^{240}Pu on the temperature-dependent reactivity behavior. The positive reactivity contribution from neutrons scattered up into the 0.3 eV resonance of ^{239}Pu tends to compensate for the negative reactivity contributions from ThO_2 Doppler broadening at increasing temperatures. As the temperature is increased above 750°C, the negative reactivity contribution from neutrons scattered up into the 1.0 eV resonance of ^{240}Pu becomes increasingly important, and when combined with the ThO_2 absorptions produces a rapid decrease in the reactivity worth.

The predictions of neutronic characteristics of plutonium-fueled HTGR lattices requires more sophisticated calculational methods than have been used for HTGR lattices fueled with either ^{235}U or ^{233}U. An improved version of GRANIT,[4] with the 35-group energy mesh from the LASER version of THERMOS (0 → 1.855 eV), was used to calculate thermal group constants for the ThO_2-PuO_2 HTGR lattice at 23, 127, 327, 527, 927, and 1327°C. Epithermal group constants were calculated at each temperature using EGGNIT.[5] The change in k_∞ as a function of temperature, calculated including upscatter above the 1.0 eV resonance of ^{240}Pu, is in better agreement with the measured shape of the temperature-dependent reactivity worth of the ThO_2-PuO_2 central cell. Comparison of calculations of k_∞ for the ThO_2-PuO_2 HTGR lattice as a function of temperature, in Figure 2.2, neglecting upscatter of neutrons above 0.683 eV and above 1.855 eV shows the increasing importance of upscatter at elevated temperatures for plutonium fueled lattices.

References

1. *D. F. Newman, "Measurement of Neutronic Parameters for a ThO_2-PuO_2 HTGR Lattice in the HTLTR,"* Technical Activities Quarterly Report, AEC Reactor Development and Technology Programs, April, May, June 1971, *BNWL-1522-3, Battelle-Northwest, October 1971.*

2. *T. J. Oakes, "Initial HTLTR Measurements with HTGR Lattice,"* Reactor Physics Quarterly Report, January, February, March 1970, *BNWL-1381-1, p. 3.16, Battelle-Northwest, May 1970.*

3. E. P. Lippincott, Measurement of the Temperature Dependence of k_∞ for a $^{233}UO_2$-ThO_2 HTGR Lattice, BNWL-1561, Battelle-Northwest, May 1971.

4. C. L. Bennett, "GRANIT: A Code for Calculating Position Dependent Thermal Neutron Spectra in Doubly Heterogeneous Systems by the Integral Transport Method," Technical Activities Quarterly Report, AEC Reactor Development and Technology Programs, July, August, September 1970, BNWL-1522-1, p. 2.48. Battelle-Northwest, October, 1970.

5. C. R. Richey, "EGGNIT: A Multigroup Cross Section Code, BNWL-1203, Battelle-Northwest, November 1969.

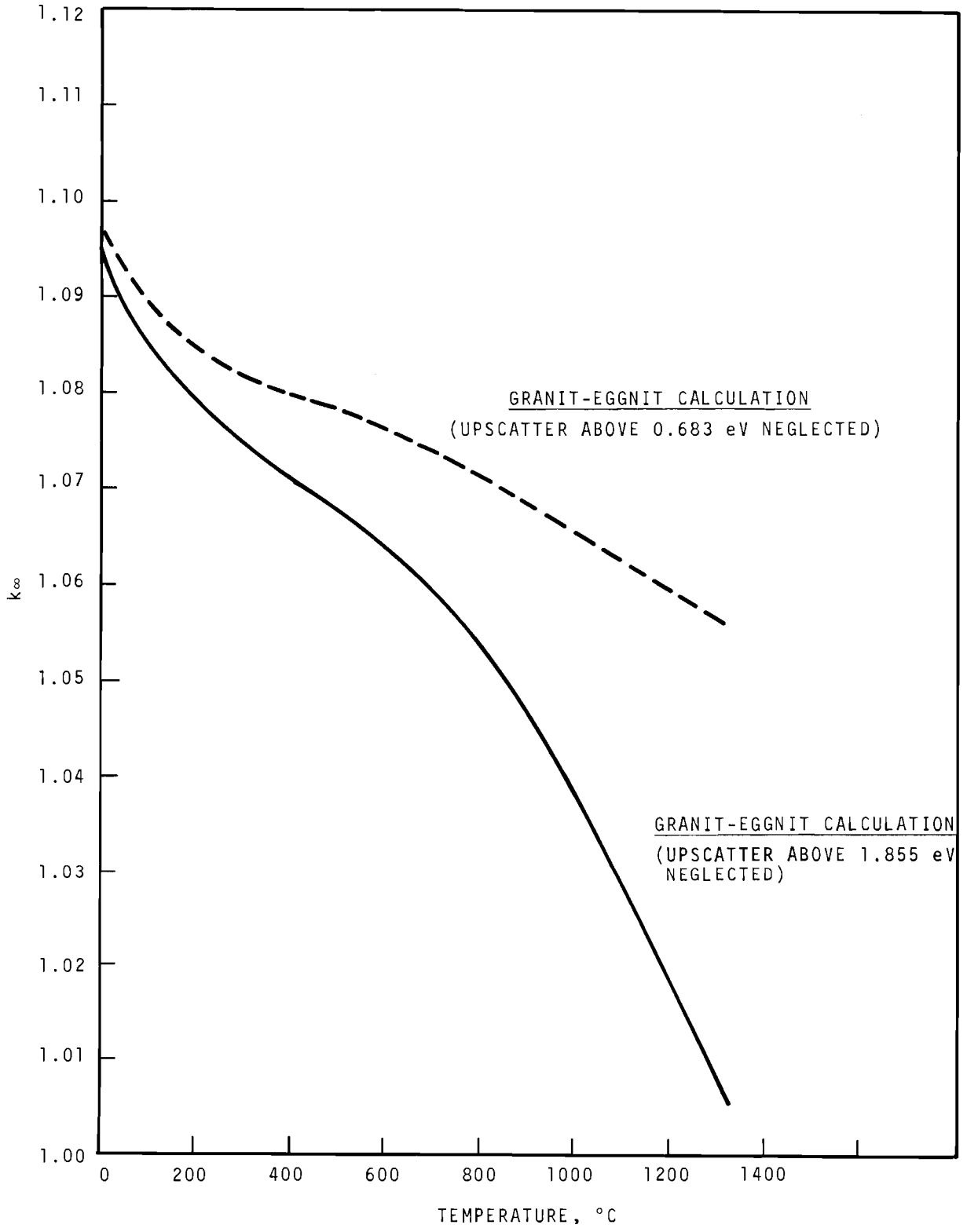

FIGURE 2.2. Calculation of k_∞ for a ThO_2-PuO_2 HTGR Lattice as a Function of Temperature

3. STEADY STATE AND TRANSIENT SUBCHANNEL CODE DEVELOPMENT AND DATA ANALYSIS

D. S. Rowe and B. M. Johnson

The objective of this study is to develop improved methods for analyzing heat transfer and fluid flow in rod bundle nuclear elements during both steady state and transient conditions. The study includes the continued development of the COBRA computer program and experiments to help verify and implement this computer program.

COBRA-III COMPUTER PROGRAM

The objective of this portion of the study is to develop improved mathematical models and computer program for predicting the steady-state and transient thermal-hydraulic performance of rod bundle nuclear fuel elements.

The major effort for this reporting period has been directed toward the continued development of an improved transverse momentum and forced crossflow mixing model for the COBRA-III computer program.

Transverse Momentum Equation

The following assumptions were used to derive the new transverse momentum equation:

- The crossflow velocity relative to the axial velocity is small at the interior of a subchannel.
- The transverse momentum flux entering a gap is equal to the transverse momentum flux emerging from a gap.

These assumptions imply that the crossflow moving from one subchannel to another loses its direction upon entering a subchannel. In other words, the vector direction of the crossflow is only considered in the gap. The vector direction of crossflows passing through a subchannel are not considered. This treatment can be justified if the crossflow velocities away from the gap are small relative to the subchannel axial velocity.

Now consider a rectangular control volume placed in the gap between two subchannels.

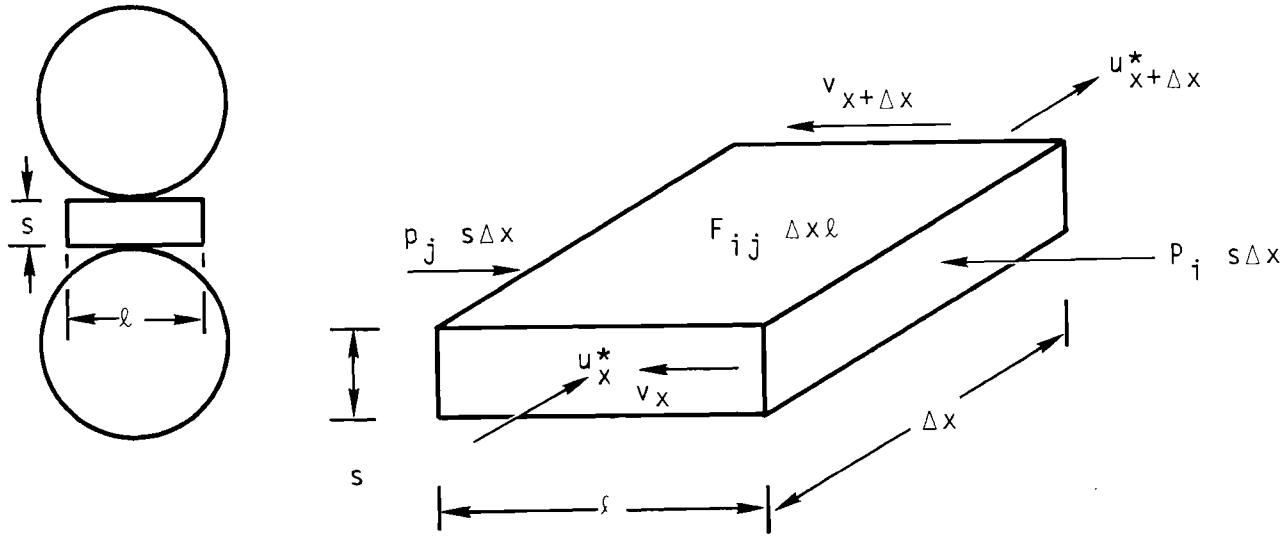

Applying the conservation of momentum equation to this control volume in the transverse direction gives

$$-F_{ij}\,\Delta x\ell - p_j\, s\Delta x + p_i\, s\Delta x = \frac{1}{g_c}\frac{\partial \rho^*}{\partial t} s\ell\Delta x v - \frac{1}{g_c}(\rho^* s\ell\, u^*\, v)_x + \frac{1}{g_c}(\rho^* s\ell\, u^*\, v)_x + (\rho^* s\ell\, u^*\, v)_{x+\Delta x}. \quad (1)$$

By rearranging this equation and taking the limit at $\Delta x \to 0$, the following equation is obtained

$$\frac{1}{g_c}\frac{\partial w_{ij}}{\partial t} + \frac{1}{g_c}\frac{\partial (u^* w_{ij})}{\partial x} = \frac{s}{\ell}(p_i - p_j) - F_{ij} \quad (2)$$

where $w_{ij} = \rho^* s v$. The F_{ij} represents the friction and form pressure loss due to crossflow. For steady flow let

$$p_i - p_j = K\frac{\rho^* v^2}{2\, g_c}. \quad (3)$$

Therefore,

$$F = \frac{K|w|w}{2s^2 g_c \rho^*} \left(\frac{s}{\ell}\right). \tag{4}$$

To put this in the form used previously in COBRA-III, let

$$F = Cw \left(\frac{s}{\ell}\right) \tag{5}$$

where $C = K|w| / 2s^2 g_c \rho^*$. The loss function, C, could have other forms based on experimental data.

By using the previous generalized form of the equations (BNWL-B-82), Equation (2) can now be written as

$$\left\{\frac{1}{g_c}\frac{\partial w}{\partial t}\right\} + \left\{\frac{1}{g_c}\frac{\partial (u^* w)}{\partial x}\right\} + \left\{\left(\frac{s}{\ell}\right) Cw\right\} = \left(\frac{s}{\ell}\right)[S]\{p\}. \tag{6}$$

The first two terms of Equation (6) can be recognized as being equivalent to the substantial derivative of the crossflow; therefore, the crossflow is carried by the flow at axial velocity, u*. This implies that once crossflows are started they tend to persist unless changed by pressure or viscous forces. This type of behavior is not contained in the earlier version of COBRA.

The parameter (s/ℓ) is new to the transverse momentum equation. From the geometry, it represents the effective ratio of the gap width to some transverse length. From Equation (6), (s/ℓ) also represents the relative importance of the inertial forces to the surface and viscous forces. The magnitude of this term will have to be determined experimentally. Tentative values of (s/ℓ) and C are being determined by analyzing selected experimental data.

Axial Momentum Equation

The axial momentum equation used is the same as in earlier versions of COBRA (BNWL-B-82) except that the axial velocity of the crossflow is assumed to be equal to the velocity of the subchannel under consideration. For a pair of subchannels the axial momentum equation can be written in the form

$$\frac{dp_i}{dx} = a_i' + \frac{1}{g_c A_i} (2u_i - u^*) w_{ij}. \quad (7)$$

The new assumption is that $u^* = u_i$; therefore,

$$\frac{dp_i}{dx} = a_i' + \frac{u_i}{g_c A_i} w_{ij} \quad (8)$$

or, in generalized form

$$\left\{\frac{dp}{dx}\right\} = \{a'\} + \left[\frac{u}{g_c A}\right]\left[S^T\right]\{w\}. \quad (9)$$

This simplification significantly improves the computation speed since it leads to the solution of symmetric matrices when solving for the crossflow. It also provides greater numerical stability. Previously, if $u^* \geq 2u_i$ the solutions were unstable.

The simplification can be justified when the crossflow velocity is small compared to the axial velocity and when adjacent subchannel velocities are rather uniform. These conditions are consistent with the assumptions made earlier for the transverse momentum equation.

Numerical Solution

Except for the momentum equations the numerical solutions are identical to those previously described for COBRA-III (BNWL-B-82).

The momentum equations are now solved without combining the transverse and axial momentum as done previously. That procedure can be used, but it does not allow diversion crossflow to be specified at selected locations within the bundle.

The new scheme uses the following difference approximation to Equation (6)

$$\left\{\frac{w(x,t+\Delta t) - w(x,t)}{g_c \Delta t}\right\} + \left\{u^*(x,t+\Delta t) \frac{w(x,t+\Delta t) - w(x-\Delta x,t+\Delta t)}{g_c \Delta x}\right\}$$

$$+ \left\{\left(\frac{s}{\ell}\right) C(x,t+\Delta t) w(x,t+\Delta t)\right\} = \left(\frac{s}{\ell}\right)[S]\left\{p(x-\Delta x,t+\Delta t)\right\}. \quad (10)$$

The pressure $\{p(x-\Delta x,t+\Delta t)\}$ is obtained from the following finite difference approximation to Equation (9)

$$\left\{\frac{p(x,t+\Delta t) - p(x-\Delta x,t+\Delta t)}{\Delta x}\right\} = \{a'\} + \left[\frac{u(x,t+\Delta t)}{g_c A(x,t+\Delta t)}\right]\left[S^T\right]\{w(x,t+\Delta t)\}. \quad (11)$$

Combining these two equations gives

$$\left\{\frac{w(x,t+\Delta t) - w(x,t)}{g_c \Delta t}\right\} + \left\{u^*(x,t+\Delta t)\ \frac{w(x,t+\Delta t) - w(x-\Delta x,t+\Delta t)}{g_c \Delta x}\right\}$$

$$+ \left(\frac{s}{\ell}\right)\{C(x,t+\Delta t)w(x,t+\Delta t)\} = \left(\frac{s}{\ell}\right)[S]\{p(x,t+\Delta t)\} - \Delta x\left(\frac{s}{\ell}\right)[S]\{a'\}$$

$$- \Delta x\left(\frac{s}{\ell}\right)[S]\left[\frac{u(x,t+\Delta t)}{g_c A(x,t+\Delta t)}\right]\left[S^T\right]\{w(x,t+\Delta t)\}. \quad (12)$$

This can be written as a set of simultaneous equations of the form

$$[A] = \{w(x,t+\Delta t)\} = \{b\} \quad (13)$$

where

$$[A] = \left[\frac{1}{g_c \Delta t} + \frac{u^*(x,t+\Delta t)}{g_c \Delta x} + \left(\frac{s}{\ell}\right)C(x,t+\Delta t)\right.$$

$$\left. + \Delta x\left(\frac{s}{\ell}\right)[S]\frac{u(x,t+\Delta t)}{g_c A(x,t+\Delta t)}\left[S^T\right]\right] \quad (14)$$

and

$$\{b\} = \left\{\frac{w(x,t)}{g_c \Delta t}\right\} + \left\{\frac{u^*(x,t+\Delta t)\ w(x-\Delta x,t+\Delta t)}{g_c \Delta x}\right\}$$

$$+ \left(\frac{s}{\ell}\right)[S]\{p(s,t+\Delta t)\} - \Delta x\left(\frac{s}{\ell}\right)[S]\{a'\}. \quad (15)$$

These equations are solved by iteration. First the values of $[S]\{p(x,t+\Delta t)\}$ are assumed equal to zero. Next, for each x, $\{w(x,t+\Delta t)\}$ is calculated by solving the set of simultaneous Equations (13) and then $[S]\{p(x,t+\Delta t)\}$ is calculated. This iteration scheme successively sweeps the calculations through the channel until the pressure difference between subchannels converges. The iteration keeps the pressure solution one iteration behind the crossflow solution.

Forced crossflow can be considered with this difference scheme by simply modifying Equation (13). Suppose the crossflow in gap ℓ is to be specified. First the right side {b} must be modified. For each k put $k \neq \ell$

$$b_{k_{mod}} = b_k - a_{k\ell}\, w_{\ell_{forced}} \tag{16}$$

and for $k = \ell$

$$b_{k_{mod}} = w_{\ell_{forced}} . \tag{17}$$

The matrix [A] is modifed by setting row ℓ and column ℓ equal to zero except $A_{\ell\ell} = 1$. As an example if $\ell = 3$ the matrix modification would be

$$\begin{bmatrix} a_{11} & a_{12} & 0 & a_{14} & \cdots & a_{1n} \\ a_{21} & a_{22} & 0 & a_{24} & \cdots & a_{2n} \\ 0 & 0 & 1 & 0 & \cdots & 0 \\ a_{41} & a_{42} & 0 & a_{44} & \cdots & a_{4n} \\ \vdots & & & & & \vdots \\ a_{n1} & & & & & a_{nn} \end{bmatrix} \cdot \begin{Bmatrix} w_1 \\ w_2 \\ w_3 \\ w_4 \\ \vdots \\ w_n \end{Bmatrix} = \begin{Bmatrix} b_1 - a_{13}\, w_{3_{forced}} \\ b_2 - a_{23}\, w_{3_{forced}} \\ w_{3_{forced}} \\ b_4 - a_{43}\, w_{3_{forced}} \\ \vdots \\ b_n - a_{n3}\, w_{3_{forced}} \end{Bmatrix} \tag{18}$$

The same procedure applies if more than one crossflow is being forced.

Wire Wrap Forced Mixing Model

The following forced crossflow mixing model has been incorporated into the latest version of the COBRA-III computer program.

Consider the wire wrap as it passes from one subchannel to another as shown in the sketch.

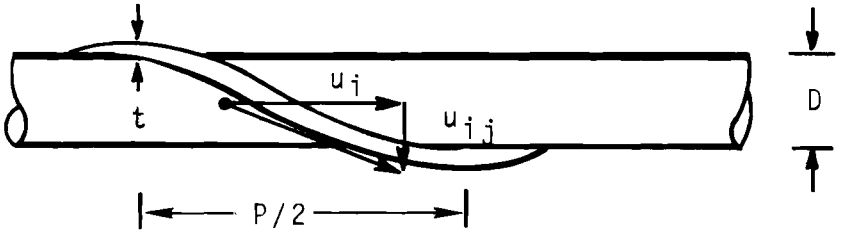

Where the wrap crosses the minimum part of the gap, the slope of the wrap imposes a transverse velocity given by

$$u_{ij} = \pi \left(\frac{D+t}{P}\right) u_i . \tag{19}$$

If this is multiplied by the fluid density and gap spacing, the crossflow per unit length becomes

$$w_{ij} = \rho_i \, s_{ij} \, u_{ij} = \pi \left(\frac{D+t}{P}\right) \left(\frac{s_{ij}}{A_i}\right) m_i . \tag{20}$$

This equation applies at the gap only. When the wrap is sufficiently far away from the gap it probably has little or no effect on forcing flow through the gap in question. It is now postulated that there is some function, f(x/P), that periodically defines the importance of Equation (20) for defining the forced crossflow through a chosen gap. This function may look something like the one in the following sketch for one wrap crossing in a gap per pitch length.

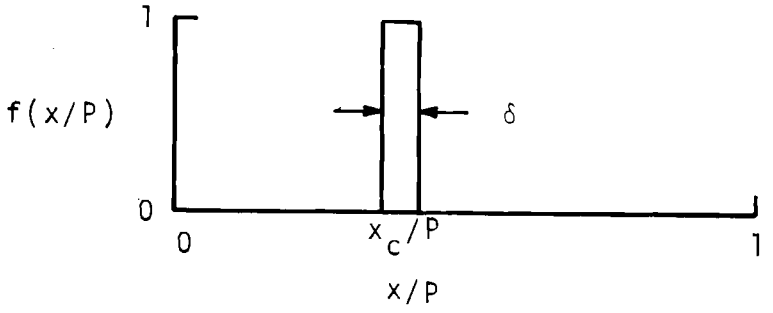

The rise in the function represents the approach of the wire toward the gap. The function peaks at 1.0 according to Equation (20) and then decays as the wrap moves away from the gap. The area under the curve represents the fraction of flow diverted through the gap as compared to the total possible flow that could be carried by a wrap over an entire pitch length. Since the shape of this function is not known, the pulse is assumed to be a rectangular pulse with width δ. The forcing function is then $f(x/P) = 0$, except for

$$f(x/P) = 1; \quad (x_c/P - \delta/2) \leq x \leq (x_c/P + \delta/2). \tag{21}$$

For computations in COBRA it is presently assumed that the flow carried through a gap by a wrap occurs within one node length, Δx, located at the point of wire wrap crossing. The total flow diverted per pulse is, therefore,

$$w\delta P = \pi \left(\frac{D+t}{P}\right) \left(\frac{s_{ij}}{A_i}\right) m_i \delta P; \quad x-\Delta x < x_o < x. \tag{22}$$

This equation shows that a fraction of the subchannel flow m_i is diverted from one subchannel to another when a wrap crosses a gap at axial position x_c when x_c lies between $x-\Delta x$ and x.

The computer calculations using this model also correct the subchannel flow area and wetted perimeter for the number of wraps in a subchannel at each axial position.

The above model has been successfully applied to forced flow mixing in a 7-pin and 19-pin bundle. Larger bundles are being considered to evaluate ability of the mixing model and numerical solution in COBRA-III to describe forced mixing in large wire wrapped bundles. Present results indicate that computer time and storage capability will not allow economical computations for bundles beyond 37-pin. Presently 19-pin calculations require about 30 minutes of UNIVAC-1108 computer time. More efficient numerical methods are needed to improve the computation time.

NOMENCLATURE

A - Subchannel area

a' - Axial pressure gradient without diversion crossflow

C - Transverse friction loss function

D - Fuel pin diameter

δ - Relative pitch length for forced crossflow pulse

F_{ij} - Transverse friction force per unit area

K - Transverse friction loss coefficient

ℓ - Effective transverse gap length

m - Subchannel mass flow rate

p - Pressure

P - Wire wrap pitch

ρ^* - Density of the diversion crossflow

s - Gap spacing

[S] - Matrix transformation that orders subchannel pair

$[S^T]$ - Transpose of [S]

t - Time

t - Wire wrap thickness

u - Subchannel velocity

u* - Axial velocity of the diversion crossflow

v - Transverse velocity in gap

w - Diversion crossflow per unit length

x - Axial distance

4. EFFECT OF ^{241}Pu ON CRITICALITY SAFETY LIMITS FOR ^{239}Pu

R. C. Lloyd

Plutonium isotopes other than ^{239}Pu are invariably present in all plutonium. The presence of these isotopes can significantly affect the criticality control limits established for ^{239}Pu. The effect on criticality of the even-neutron nuclides such as ^{240}Pu and ^{242}Pu is to cause the critical dimensions and masses for the isotopic mixture to be greater than that for ^{239}Pu alone. The effects are strongly dependent on the neutron spectrum and any moderating diluent that may be present, such as water. The highly fissile odd-neutron nuclide ^{241}Pu will cause significant reductions in the critical dimensions and masses below that of ^{239}Pu. The minimum critical mass for ^{241}Pu has been calculated to be only 260 g for a concentration of 32 g/ℓ in water, and the limiting critical concentration for this nuclide in water is only about 5 g/ℓ.[1]

A series of experiments has now been completed with plutonium obtained from high burnup fuel to establish the combined effects of the various isotopes of plutonium on criticality. The experiments were performed in a 24-inch diameter, water-reflected, cylindrical vessel. Ten data points have been obtained with critical heights and masses being determined for various plutonium concentrations and nitric acid molarities in the plutonium nitrate solutions. Plutonium concentrations covered the range of about 40 to 140 g Pu/ℓ with nitric acid molarities ranging from about 1.5 to 5. A recent (August 11, 1971) isotopic analysis of the plutonium used yielded the following results:

^{238}Pu - 0.203 ± 0.014 wt%

^{239}Pu - 41.362 ± 0.177 wt%

^{240}Pu - 42.886 ± 0.143 wt%

^{241}Pu - 10.884 ± 0.140 wt%

^{242}Pu - 4.705 ± 0.084 wt%

The data from the criticality experiments (conducted during August 9-19, 1971) with this plutonium have been reduced, yielding critical volumes and masses for the plutonium nitrate solutions used in the 24-inch diameter, water-reflected, cylindrical vessel. The results are given in the following tabulation:

Data from Critical Experiments
on High Burnup Plutonium Solutions

Pu Concentration, g/ℓ	Nitric Acid Molarity	Critical Height in 24-in. Diam. Cylinder, cm	Critical Volume, ℓ	Critical Mass, kg
140.0	5.02	54.1	158.3	22.16
116.0	4.14	50.5	147.9	17.16
99.26	3.67	48.3	141.2	14.02
85.53	3.12	47.0[(a)]	137.48	11.75
85.53	3.12	47.3[(a)]	138.35	11.83
75.64	2.74	47.3	138.32	10.46
65.12	2.41	49.1	143.71	9.36
56.34	2.05	52.8	154.51	8.71
46.83	1.70	63.5	184.65	8.69
40.58	1.46	80.9	236.71	9.61

a. *Shows effect on critical height if external water reflection is maintained at same height as Pu solution as opposed to the vessel fully immersed in water.*

Correlation of the experimental data and calculational methods are in progress using the KENO Monte Carlo Code. When calculations are completed they will provide an integral check on the cross sections and computational codes used.

Reference

1. *E. D. Clayton and S. R. Bierman, "Criticality Problems of Actinide Elements," Actinides Reviews, Vol. 1, No. 5, pp. 409-432, September 1971.*

5. NUCLEAR GRAPHITE

G. L. Tingey

IN-REACTOR CREEP

W. J. Gray

Constant-stress irradiation creep experiments are being conducted to high fluences (up to 2.5×10^{22} n/cm^2, E > 0.18 MeV) to determine whether any change in creep behavior occurs following the onset of rapid expansion at high fluences. Capsules containing graphite samples under compressive stresses are being irradiated at 550 and 800°C. A third capsule containing samples under tensile stresses is being irradiated at 800°C. A fourth capsule is planned which will contain samples under compressive stresses and will operate at about 1100°C. This capsule is scheduled to be charged into the reactor about February 1972.

The first three capsules were shipped to Idaho Falls in June for charging into the ETR reactor. Because of some problems with the reactor, however, charging was delayed until September. The tensile creep capsule will be discharged in November after one cycle of irradiation. The fluence for these samples, which are being irradiated for the first time, will then be about 1.5×10^{21} n/cm^2 (E > 0.18 MeV). The two compressive creep capsules will be discharged in February, at which time the maximum fluence received by the samples will be about 1.0×10^{22} n/cm^3 (E > 0.18 MeV).

RADIOLYTIC REACTIONS IN GRAPHITE MODERATED REACTORS

R. P. Turcotte and G. L. Tingey

The radiolytic reaction of carbon monoxide and water vapor has now been investigated at six different equimolar concentrations between limits of 10 and 940 vpm in one atmosphere helium. During the last quarter, results at 100, 240, and 465 vpm were obtained by the continuous flow, chromatographic technique. The data were fit to equations of the form G (molecules/100 eV) = $aT^{1/2}\ e^{-E/RT}$ to yield the constants given in Table 5.1 (earlier results are included). The $\ln(G/T^{1/2})$ versus 1/RT plots from which activation energies were determined are shown in Figures 5.1 and 5.2 for

CO_2 and H_2, respectively. In addition, isothermal product yields have been determined at approximately 125°C and approximately 460°C. The curves are shown for 125°C in Figure 5.3, but are somewhat tentative pending more data in the 400 to 1000 vpm region.

TABLE 5.1. Constants a and E for the Equation $G = aT^{1/2} e^{-E/RT}$ as a Function of Reactant Concentration

$[H_2O] = [CO]$ vpm	a		-E(Kcal)	
	H_2	CO_2	H_2	CO_2
940	0.061	0.150	0	0
465	0.030	0.192	1.5	0.3
240	0.018	0.085	1.5	1.0
100	0.008	0.061	1.7	1.0
65	0.004	0.014	1.6	1.1
10	0.004	0.005	1.6	1.6

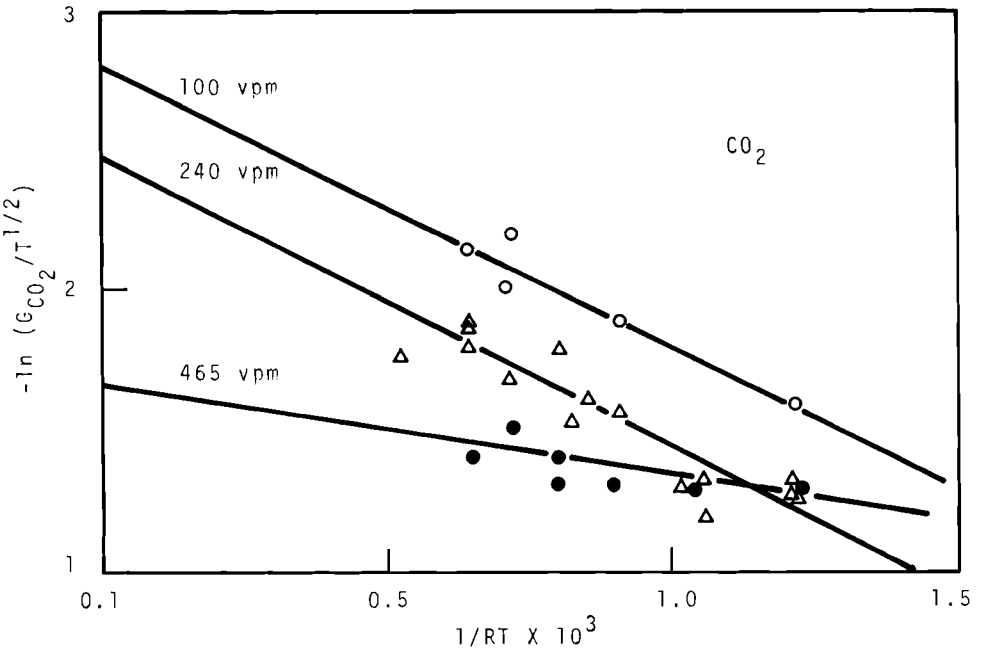

FIGURE 5.1. Plot of $\ln(G_{CO_2}/T^{1/2})$ Versus 1/RT for Various Equimolar (CO, H_2O) Concentrations

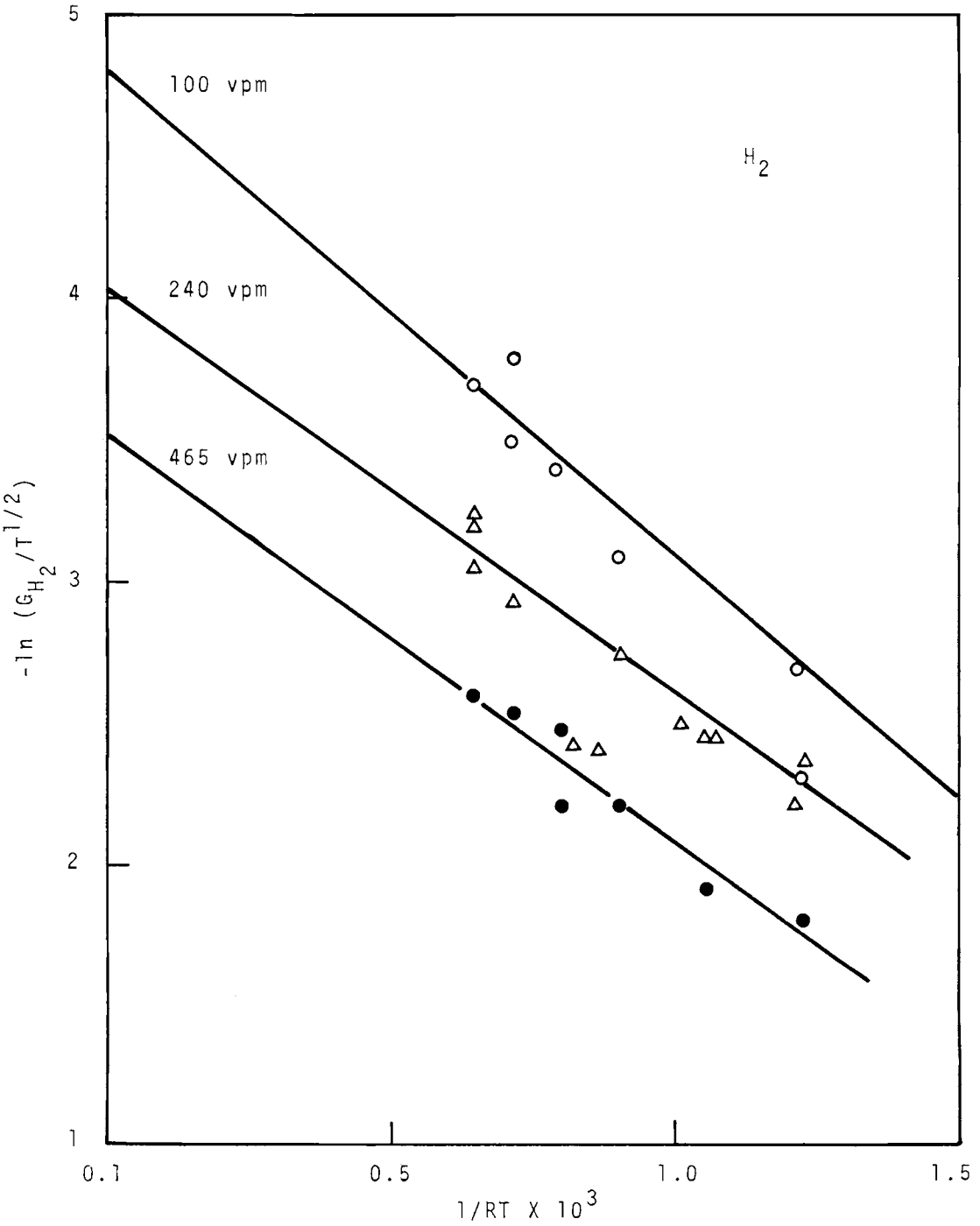

FIGURE 5.2. Plot of $\ln(G_{H_2}/T^{1/2})$ Versus 1/RT for Various Equimolar (CO, H_2O) Concentrations

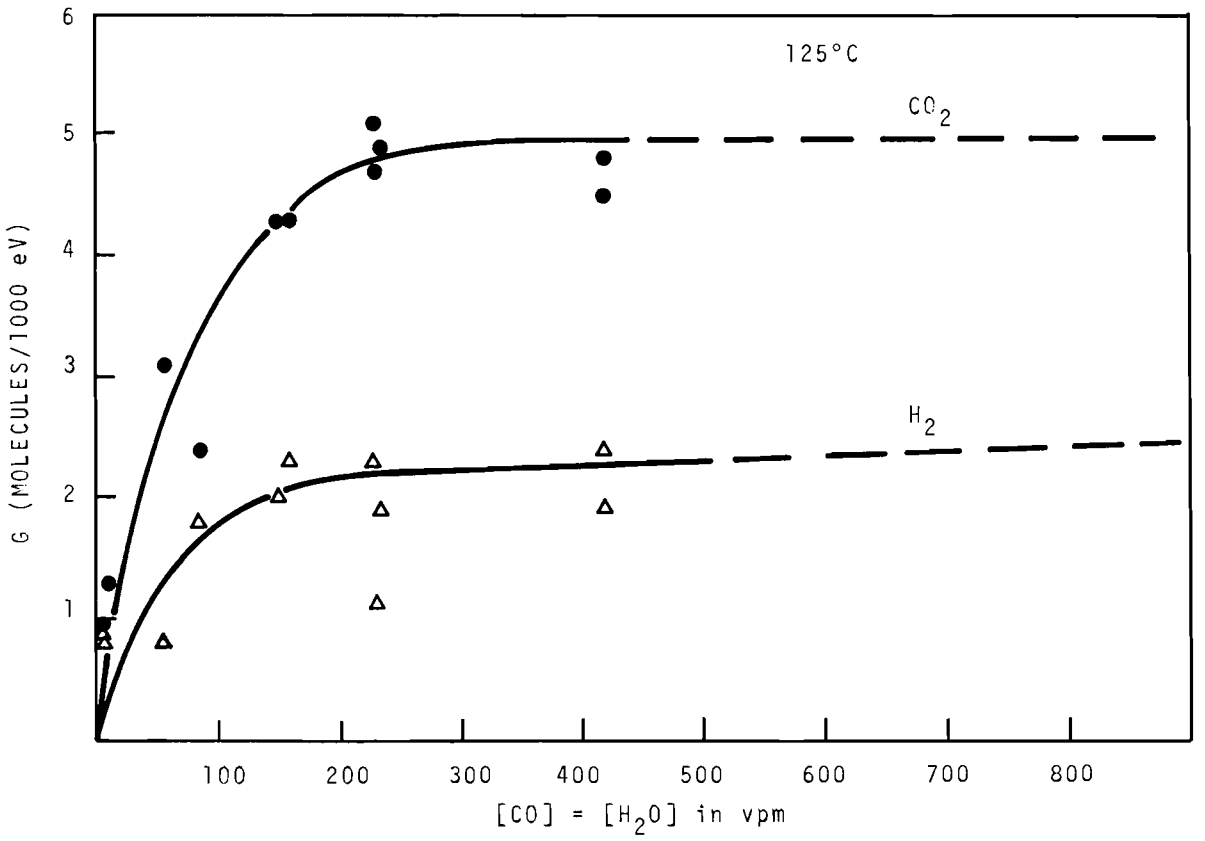

FIGURE 5.3. Product Yields (G) for H_2 and CO_2 as a Function of Equimolar (CO, H_2O) Concentrations

The additional results confirm negative activation energies for the reaction at these high dilutions and although scatter is quite high, a regular decrease in the constants (a) and E (at least for CO_2) are observed with decreasing reactant concentration as shown in Table 5.1.

The oxygen impurity problems discussed previously have not been remedied. Rather, the system has been improved to the point that air in-leakage is essentially zero and it is now certain that some product of radiolysis at lower temperatures (presumably a solid carbon suboxide) decomposes when heated to substantially increase oxygen levels. For example, following prolonged flow of the CO, H_2O mixture at 125°C, rapid heating to approximately 500°C causes an increase in oxygen concentration from <0.3 vpm to as high as 30 vpm which passes through a maximum and decays to low levels

only after several hours (depending on flow rates, etc.). Most of the present data were taken with decreasing temperature to reduce this problem, but variation in flow rates and oxygen partial pressures for the various dilutions undoubtedly alter real oxygen pressures within the cell. Deposition and variation of solid material and variation in oxygen levels seem virtually impossible to control and may well explain the somewhat high scatter in the data. In general, O_2 levels did not exceed 2 vpm in the effluent gas. This level is, however, comparable to product concentrations and for the very low reactant concentrations especially, the results should be considered with this problem clearly in focus.

EFFECT OF SAMPLE SIZE ON DIMENSIONAL STABILITY OF GRAPHITE

W. J. Gray

The study of the size-effect problem has been expanded to include an investigation of a phenomenon called "cold-seeding," wherein graphite samples are briefly irradiated at low temperatures prior to the normal high-temperature irradiation. A large number of samples which have been previously "cold-seeded" are currently being irradiated to high fluences at high temperatures in the ETR.

The cold-seeding capsule has been shipped to Idaho Falls for charging into the ETR in November for the third period of high-temperature irradiation. Results from the second irradiation period have been reported previously.[1]

HIGH TEMPERATURE IRRADIATIONS

W. J. Gray and W. C. Morgan

Capsule GEH-13-422 was inserted in the ETR at the beginning of Cycle 113; the capsule is controlling normally, with the highest sample temperatures at 1400°C. It is planned to continue irradiation of this capsule through ETR Cycle 115, with discharge expected during April 1972.

MECHANISM OF IRRADIATION DAMAGE

W. C. Morgan and W. J. Gray

A report[2] on the irradiation-induced changes in glassy carbons has been issued and submitted to Carbon. As a result of a similar study on the irradiation-induced changes for pyrocarbons, Bokros et al.[3] had concluded that although the apparent crystallite size, L_c, tends to decrease for carbons with initial L_c values greater than about 50 Å, irradiation tended to increase the L_c value for carbons having smaller initial L_c values. This conclusion was interpreted[4] as furnishing support for the existence of an equilibrium state of disorder, characterized by L_c values near 50 Å, and an irradiation-induced ordering (improvement in crystallite perfection and density) of initially poorly ordered carbons.

Our results on glassy carbons do not support the hypothesized equilibrium state of disorder, characterized by L_c values near 50 Å. Re-examination of the data presented by Bokros et al.[3,4] lead us to conclude that the increase in L_c observed by Bokros et al. was quite likely due to an annealing change, superimposed on the normal irradiation-induced decrease in L_c.

Thus, we can conclude that the irradiation-induced changes in the low-temperature pyrocarbons are compatible with changes in glassy carbons and with previous results on other carbon materials in that the primary effect of irradiation is to decrease the crystallite perfection and crystallite density.[5] Moreover, if an equilibrium state of disorder exists, our results suggest that the associated L_c value is not greater than 16 Å.

References

1. *Technical Activities Quarterly Report, AEC Reactor Development and Technology Programs, April, May, June 1971, BNWL-1522-3, Battelle-Northwest, September 1971.*
2. *W. J. Gray, W. C. Morgan, J. H. Cox and E. M. Woodruff, Irradiation-Induced Length Changes of Glassy Carbon, BNWL-SA-3985, Battelle-Northwest, July 29, 1971.*
3. *J. C. Bokros and R. J. Price, Carbon. Vol. 4, p. 441, 1966.*
4. *J. C. Bokros, R. J. Price and K. Koyama, Carbon. vol. 4, p. 293, 1966.*
5. *W. C. Morgan, Carbon, vol. 5, p. 85, 1967.*

6. PHOENIX FUEL STUDIES

R. I. Smith

DOCUMENTATION

A document[1] has been issued which describes the program of critical experiments conducted at the loading of the Phoenix fuel core into MTR, the measured variations of some of the reactor physics parameters with fuel burnup, and the burnup history of the core while in MTR. The results are compared, where possible, with results from the PRCF-Phoenix experiment[2] and with pre-experiment calculations.[3]

Preparation of the final report on the MTR-Phoenix fuel experiment is in progress.

DATA COLLECTION

Thirty-six fuel plates from nine different elements were gamma scanned to obtain axial and lateral burnup profiles. Two samples were cut from each of two fuel plates for isotopic analysis. One pair of samples represented the interior of the core (asymptotic region) and the other pair of samples represented the core boundary region. The results of the destructive analysis are listed in Table 6.1. Plate 22-8 was from the asymptotic region and plate 3-8 was from the boundary region.

Six flux monitor wands were also studied, five irradiated and one unirradiated. Of the irradiated wands, two were removed from the core at intermediate levels of burnup, and the remaining three wands were removed at the end of the core life. Five wands were gamma scanned to obtain axial burnup profiles. Samples were cut from two irradiated wands and one unirradiated wand for isotopic analysis. The results from the destructive analysis of flux monitor wands are given in Table 6.2.

The isotopic data from the two fuel plates have been fitted using DBUFIT[5] to obtain ratios of effective cross sections for the plutonium isotopes. It was necessary to fix two of the parameters to achieve a fit. The parameters chosen to be fixed were $\hat{\sigma}_a^{241}/\hat{\sigma}_a^{239}$ and $\hat{\sigma}_a^{242}/\hat{\sigma}_a^{239}$, and a

TABLE 6.1. Summary of Destructive Analysis of Fuel Plate Samples

	Beginning of life atom Concentration (BOL)[a]	End of Life Atom Concentration (EOL)[b,c]			
		Plate 22-8		Plate 3-8	
Sample No.	W 1126	W-1429	W 1679	W 1430	W 1680
^{238}Pu	0.539	0.7091	0.6855	0.6987	0.6979
^{239}Pu	66.516	48.84	50.78	41.39	44.17
^{240}Pu	23.201	24.04	24.09	25.02	25.18
^{241}Pu	6.488	9.344	9.004	8.892	8.477
^{242}Pu	3.257	3.688	3.641	4.085	3.962
Total	100.00	86.62	88.20	80.09	82.50
Atom % Burnup (BOL-EOL)	0	13.38	11.80	19.92	17.50

a. BOL = atoms of isotope per 100 initial atoms of plutonium at beginning of life (1-28-70).

b. EOL = atoms of isotope per 100 initial atoms of plutonium at end of life (4-23-70).

c. Values derived using measured isotopic ratios and ^{148}Nd analysis results in ISODIL.(4)

TABLE 6.2. Summary of Destructive Analysis of Flux Wand Samples

	Beginning of life atom Concentration (BOL)[a]	End of Life Atom Concentrations (EOL)[b,c]					
		Wand #12			Wand #8		
Sample No.	W 1126	W 1130	W 1131	W 1132	W 1127	W 1128	W 1129
^{238}Pu	0.539	0.5788	0.6147	0.6394	0.6148	0.6585	0.6819
^{239}Pu	66.516	58.94	52.58	47.93	54.31	45.10	42.67
^{240}Pu	23.201	23.13	22.93	22.42	22.94	22.41	21.94
^{241}Pu	6.488	8.227	9.612	10.63	8.999	10.76	11.26
^{242}Pu	3.257	3.441	3.629	3.797	3.556	3.932	4.023
Total	100.00	94.32	89.37	85.42	90.42	82.86	80.58
Atom % Burnup (BOL-EOL)	0	5.68	10.63	14.58	9.58	17.14	19.42

a. BOL = atoms of isotope per 100 initial atoms of plutonium at beginning of life (1-28-70).

b. EOL = atoms of isotope per 100 initial atmos of plutonium at end of life (4-23-70).

c. Values derived using measured isotopic ratios and ^{148}Nd analysis results in ISODIL.[4]

study was performed to determine the sensitivity of the fits to the values of these fixed parameters. The results of these analyses are given in Table 6.3.

There are significant differences in the values of most of the parameters between the asymptotic region (plate 22-8) and the boundary region (plate 3-8), thus emphasizing the fact that a zero-dimensional burnup calculation is not adequate for cores like the MTR-Phoenix.

References

1. *J. W. Kutcher and E. C. Davis, The MTR-Phoenix Fuel Experiment: Critical Test and Burnup Results, BNWL-1593, Battelle-Northwest, 1971.*

2. *E. C. Davis, R. I. Smith and L. D. Williams, Critical Experiments in an MTR Mockup Using Phoenix Fuel, BNWL-1481, Battelle-Northwest, 1970.*

3. *C. M. Heeb, Analysis of the Phoenix Fuel Experiments, BNWL-1514, Battelle-Northwest, 1970.*

4. *R. P. Matson, ISODIL, A Computer Code for Processing Isotopic Dilution Measurements from Spent Fuel Samples, BNWL-1555, Battelle-Northwest, 1971.*

5. *R. P. Matsen, DBUFIT-I, A Least Squares Analysis Code for Nuclear Burnup Data, BNWL-1386, Battelle-Northwest, 1970.*

TABLE 6.3. Summary of DBUFIT Analysis of Fuel Plate Samples

DBUFIT Case No.	Material and Data	Cross-Section Ratios				(Fixed)	Quality of fit[a]
		α^{239}	$\hat{\sigma}_a^{240}/\hat{\sigma}_a^{239}$	$\hat{\sigma}_a^{241}/\hat{\sigma}_a^{239}$	α^{241}	$\hat{\sigma}_a^{242}/\hat{\sigma}_a^{239}$	χ^2/d.f.
56-1	Plate 22-8	0.524 ± 0.005	0.713 ± 0.003	0.950 fixed	0.440 ± 0.014	0.260	0.153
56-2	do	0.557 ± 0.005	0.747 ± 0.003	1.050 fixed	0.382 ± 0.012	0.260	0.162
56-3	do	0.592 ± 0.006	0.782 ± 0.003	1.150 fixed	0.337 ± 0.011	0.260	0.172
57-1	do	0.558 ± 0.005	0.748 ± 0.003	1.050 fixed	0.359 ± 0.011	0.230	0.140
57-2	do	0.556 ± 0.006	0.747 ± 0.003	1.050 fixed	0.405 ± 0.013	0.290	0.187
56-4	Plate 3-8	0.434 ± 0.012	0.490 ± 0.006	0.900 fixed	0.459 ± 0.032	0.120	1.34
56-5	do	0.464 ± 0.012	0.522 ± 0.006	1.000 fixed	0.395 ± 0.026	0.120	1.34
56-6	do	0.496 ± 0.013	0.554 ± 0.006	1.100 fixed	0.346 ± 0.022	0.120	1.34
57-3	do	0.465 ± 0.012	0.522 ± 0.006	1.000 fixed	0.377 ± 0.025	0.100	1.33
57-4	do	0.464 ± 0.012	0.522 ± 0.006	1.000 fixed	0.413 ± 0.027	0.140	1.35

a. Values of chi squared divided by the degrees of freedom which are reasonably close to unity are expected for a satisfactory fit and reasonable uncertainties. Significantly smaller values indicate uncertainties on data points have been overestimated and the fit is better than expected.

7. PUBLICATIONS AND PRESENTATIONS

DOCUMENTS PUBLISHED

Shojiro Matsuura, D. L. Prezbindowski, Analytical Correlations of: PRTR Batch Core Experiment, BNWL-B-113, June 1971. (Limited Distribution)

A. L. Pitner, High Temperature Irradiations (1000-1300°C) on a Variety of Graphites to Exposures > 10^{22} n/cm^2. BNWL-1540, July 1971.

G. F. Shiefelbein and R. E. Lerch, Dissolution Properties of UO_2-PuO_2 Thermal Reactor Fuels, BNWL-1581, June 1971.

B. R. Leonard, Jr., Thermal Cross Sections of the Fissile and Fertile Nuclei for ENDF/B-II, BNWL-1586, June 1971.

D. R. Oden, Comparison of Calculated and Measured Values of ρ^{28} and δ^{28}_{25} for 26 Lattices of UO_2 Rods in a Light Water Moderator, BNWL-1589, May 1971.

J. W. Kutcher and E. C. Davis, The MTR-Phoenix Fuel Experiment: Critical Test and Burnup Results, BNWL-1593, June 1971.

T. J. Oakes, Measurement of k_∞ as a Function of Temperature for a $^{233}UO_2$-$^{232}ThO_2$-C Lattice, BNWL-1601, June 1971.

D. R. Oden, G. D. Seybold, "DRAFT: A Computer Code for the Calculation of Fission Product Activity Ratios," BNWL-1607, July 1971.

A. D. Vaughn, Study of the Reactivity Effects of Finite PuO_2 Particle Sizes in Mixed PuO_2-UO_2 Nuclear Fuels, BNWL-1608, August 1971.

G. D. Seybold, BNW Program NOISE, BNWL-1609, July 1971.

A. D. Vaughn and D. E. Christensen, Installation and Testing of a Spent Fuel Age Monitor at NPD, BNWL-1594, July 1971.

JOURNAL ARTICLES PUBLISHED

D. A. Kottwitz, "Parallel Beams of Neutrons or X-rays by Multiple Bragg Reflection," Acta Cryst., Vol. A 27, 391 (Sept. 1971).

E. D. Clayton and S. R. Bierman, "Criticality Problems of Actinide Elements," Actinides Reviews, Vol. 1, No. 5, (September 1971).

JOURNAL ARTICLES ACCEPTED FOR PUBLICATION:

M. D. Freshley and L. J. Harrison, "The Transient Behavior of Vipac and Pellet Thermal Reactor Oxide Fuels," BNWL-SA-3982, July 1971. Submitted to Nuclear Technology.

M. D. Freshley, "Mixed-Oxide Fuel Irradiations in PRTR," BNWL-SA-3981, July 1971. Submitted to Nuclear Technology.

JOURNAL ARTICLES SUBMITTED

R. P. Matsen, "The Determination of Ratios of Effective Cross Sections from Measured Burnup Data for Yankee Rowe, BNWL-SA-4075, Submitted for publication in Nuclear Technology, September 1971.

L. G. Faust, L. W. Brackenbush, R. C. Smith, L. L. Nichols and D. W. Brite, "Radiation Dose Rates from UO_2-PuO_2 Thermal Reactor Fuels, BNWL-SA-3661, Submitted for publication in Nuclear Technology, September 1, 1971.

PRESENTATIONS

Summaries Published in Trans. Am. Nucl. Soc. Vol. 14. No. 2, (1971):

U. P. Jenquin, L. D. Williams, W. C. Wolkenhauer, "An Experimental/Calculational Comparison for 14-MeV Neutrons in Graphite," p. 447.

C. L. Brown, L. C. Davenport, E. D. Clayton, "Subcritical Experiments with Mixed-Oxide Fuels of Plutonium and Uranium in Poisoned Lattices," p. 675.

C. L. Brown, "Criticality Safety Considerations in the Fabrication of UO_2 and PuO_2-UO_2 Fuels for Light-Water Reactors," p. 681 (invited paper).

C. L. Brown, L. C. Davenport, "Criticality Safety Considerations in the Design of a Large Concrete Storage Array for Plutonium Oxide-Uranium Oxide Fuel Subassemblies, p. 683.

L. C. Schmid, N. E. Carter, U. P. Jenquin, B. R. Leonard, Jr., W. C. Wolkenhauer, "Status of Reactor Physics Technology Related to Pu-Recycle Fuel Licensing," p. 822. (Invited paper).

D. F. Newman, "Reactivity Effect of PuO_2 Particulate Fuel," p. 828.

M. D. Freshley, "Thermal Reactor Mixed-Oxide Fuel Performance," pp. 563-565.

DISTRIBUTION

No. of Copies

OFFSITE

2 AEC Chicago Patent Group

G. H. Lee

10 AEC Division of Reactor Development and Technology

Asst. Dir. for Project Management
Chief, Water Project Branch (2)
Chief, Gas Cooled Projects Branch
Asst. Dir. for Reactor Technology
Chief, Reactor Physics Branch (2)
Chief, Core Design Branch
Chief, Fuels and Materials Branch (2)

1 AEC Division of Nuclear Materials Safeguards

H. Werner

1 AEC Division of International Affairs

M. B. Kratzer

1 AEC Division of Materials Licensing

R. H. Odegaarden

1 AEC Division of Naval Reactors

A. Radkowsky

1 AEC Division of Production

F. P. Baranowski

3 AEC Division of Reactor Licensing

R. E. Baker
R. E. Ireland
P. A. Morris

2 AEC Division of Reactor Standards

E. G. Case

1 AEC Division of Research

G. A. Kolstad

226 AEC Division of Technical Information Extension

1 AEC Division of Waste Management and Transportation

F. K. Pittman

1 AEC Savannah River Operations Office

R. Thorne

No. of Copies

2 Aeroject Nuclear Corp.
P.O. Box 1845
Idaho Falls, Idaho 83401

R. M. Brugger
R. A. Grimesey

6 Argonne National Laboratory

Reactor Physics Constants Center (2)
R. Avery
C. H. Bean
P. Gast
R. E. Macherey

5 Atomic Energy of Canada Limited
Chalk River, Ontario, Canada

D. H. Charlesworth
M. Duret
C. Millar
L. Pease
H. K. Rae

2 Atomic Energy Establishment
Dragon Project
Winfrith, Dorchester,
Dorset, England

M. R. Everett
H. Gutmann

3 Atomics International

H. Alter
N. Ketzlach
Liquid Metals Engineering Center (LMEC)

1 Australian Atomic Energy Commission
AAEC Research Establishment
Private Mail Bag, Sutherland 2232
N.S.W., Australia

Dr. J. L. Symonds
Chief, Physics Division

1 Battelle Memorial Institute
Columbus, Ohio

Roger Merrill

No. of Copies

4 Babcock and Wilcox Company
161 E. 42nd Street
New York, N. Y. 10017

H. M. Jones
D. H. Roy
J. Tulenko
W. A. Wittkopf

1 Bechtel Corporation
Vernon, California

M. Aronchick

1 Bettis Laboratory, Westinghouse Electric Company

J. J. Taylor

2 Bhabha Atomic Research Centre
Trombay, Bombay-85, India

S. R. Dwivedi, Theoretical Physics Section/RED
Central Complex Bldg.
J. K. Bahl, Metallurgy Division
Modular Laboratories

3 Brookhaven National Laboratory

J. Chernick
H. Kouts
S. Pearlstein

1 California Institute of Technology

H. Lurie, Engineering Div.

1 Catholic University of America
Dept. of Nuclear Sci. & Eng.
Washington, D.C.

G. L. Simmons

10 C.E.N - Saclay
Boite Postale 2
Gif-Sur-Yvette (S et O), France

B. LaPonche
P. Lecorche
G. Vendryes

1 CNEN - Casaccia
00060 - S. Maria Di Galeria
Rome, Italy

Paolo Loizzo

No. of Copies

2 CNEN-Centro Studi-Nucleaire
Casaccia, Rome, Italy

Ugo Farinelli
Augusto Gandini

3 Combustion Engineering, Nuclear Division
Windsor, Connecticut

W. P. Chernock
R. Harding
S. Visner

1 Consumers Power Company
Jackson, Michigan

G. T. Walke

2 Cornell University
Ithaca, N. Y.

R. T. Cuykendall, Eng. Physics
M. Nelkin

2 Assoc. C.E.N. Belgo Nucleaire
35 Rue Des Colonies, Belgium

H. Bairiot
L. Bindler

1 Duke University
Durham, N. C.

W. J. Seeley, School of Eng.

1 Ebasco Services, Inc.
2 Rector Street
New York, N. Y. 10006

D. R. de Boisblanc

2 Edison Electric Institute
90 Park Ave.
New York, N. Y. 10017

John J. Kearney (2)

5 E. I. du Pont de Nemours & Co., Inc.
Savannah River Laboratory

H. K. Clark
J. L. Crandall
G. Dessauer
E. J. Hennelly
H. Honeck

No. of Copies	
1	ENEL Via G. B. Martini (Pizaaz Verdi) Rome, Italy Mr. Paoletti Gualandi
10	EURATOM 53, Rue Billiard Brussels 4, Belgium A. de Stordeur
1	FFR - AB Atomenergi Studsvik, Pa NYKOPING Sweden Evelyn Sokolowski
2	General Electric Company Knolls atomic Power Laboratory R. Ehrlich C. Lubitz
7	General Electric Company San Jose, CA R. L. Crowther M. R. Egan D. L. Fischer P. Greebler S. Levy R. B. Richards T. M. Snyder
1	General Electric Company Nucleonics Laboratory H. W. Alter
1	General Electric Company Vallecitos Atomic Laboratory B. F. Judson
8	Gulf General Atomic W. E. Bell R. C. Dahlberg G. B. Engle T. R. Moffett J. M. Neill C. A. Perty H. B. Stewart R. F. Turner

No. of Copies

2 Gulf United Nuclear Corporation
Elmsford, N. Y. 10523

T. B. Holden
J. R. Tomonto

1 Istanbul Technical University
Giimiis, Suyer, Istanbul, Turkey

Director, Nuclear Energy Institute

1 Japan Atomic Energy Research Institute (JAERI)
Tokaimura, Naka-gun, Ibarakiken, Japan

Shunya Nozawa

1 Japan Atomic Energy Institute (JPDR-TCA)
Tokaimura, Ibarakiken, Japan

Shojiro Matsuura

1 Kernforschungszentrum Karlsruhe
7500 Karlsruhe, Germany

Professor W. Haefele

1 Kerr-McGee
Oklahoma City, Oklahoma

Parker S. Dunn

3 Los Alamos Scientific Laboratory, Box 1663

G. H. Best
G. E. Hansen
M. C. Smith

1 Manhattan College
Riverdale, New York, N. Y.

Brother Gabriel Kane

2 Massachusetts Institute of Technology

Irving Kaplan
D. D. Lanning

1 Mitshubishi Corp.
Nuclear Power Section
6-3, Marunouchi
Chiyoda-Ku, Tokyo, Japan

Setsuo Kobayashi

1 North American Aviation Science Center

E. R. Cohen

1 North Carolina State College

R. L. Murray

No. of Copies

2 Nuclear Fuels Services, Inc.
Suite 600
6000 Executive Blvd.
Rockville, Maryland 02852

R. Deuster
R. E. L. Stanford

1 NUKEM
D-645, NANAU
POSTFACH 869
Germany

Wolfgang K. L. Jager

6 Oak Ridge National Laboratory

J. H. de Nordwell
W. P. Eatherly
R. R. Kasten
R. C. Maienschein
A. M. Perry
M. W. Rosenthal

1 Pakistan Institute of Nuclear Science & Technology
P. O. Nilore, Rawalpindi, Pakistan

M. A. Mannan

1 Penn State College

W. F. Witzig

1 Pennsylvania State University
University Park, Pennsylvania

P. L. Walker, Jr.

1 Philadelphia Electric Company
1000 Chestnut Street
Philadelphia 5, Pa.

Wayne C. Astley

1 Phillips Petroleum Company
Idaho Falls, Idaho

W. B. Lewis

1 Power Reactor and Nuclear Fuel Development Corp.
Narita, O-ARAI, Higashi-Ibarbaki-Gun, Ibaraki-Ken, Japan

Hjime Sakata

1 Purdue University

P. N. Powers, Nucl. Eng. Dept.

1 Rensselaer Polytechnic Institute

E. R. Gaerttner

No. of Copies

1 S. C. K. - C. E. N.
BRL,
Mol-Donk, Belgium

Dr. H. Vanden Broeck

2 Tennessee Valley Authority
310 Power Bldg.,
Chattanooga, TE 37408

H. B. Brooks
R. H. Davidson

1 Union Carbide Corporation (ORNL)

E. B. Johnson

2 United Kingdom Atomic Energy Agency
Atomic Weapons Research Establishment
Aldermaston, Berkshire, UK

R. C. Lane (1)

Authority Health and Safety Branch,
Safeguards Division, Risley,
Warrington, UK

J. H. Chalmers (1)

2 United Kingdom Atomic Energy Authority
Atomic Energy Research Establishment - Harwell
Didcot, Berkshire, England

J. H. W. Simmons
John Wright

2 United Kingdom Atomic Energy Authority
General Reactor Physics Division
Winfrith, England

Dr. J. G. Tyror
C. G. Campbell

1 University of Arizona
Tucson, Arizona

Monte V. Davis, Nucl. Eng. Dept.

1 University of California
Department of Nuclear Engineering

V. E. Schrock

1 University of Florida
Gainesville, Florida

R. E. Uhrig, Nucl. Eng.

No. of Copies

1 University of London Reactor
Silwood Park, Sunninghill,
Ascot, Berkshire, England

D. MacMahon

1 University of Minnesota
Minneapolis, Minnesota

H. S. Isben, Chem. Eng. Dept.

1 University of Nevada
Reno, Nevada

T. V. Frazier, Physics Dept.

1 University of Notre Dame
Notre Dame, Indiana

E. W. Jerger, Dept. of Mech. Eng.

2 University of Tennessee
Knoxville, Tennessee

A. H. Nielsen, Physics Dept.
P. F. Pasqua, Nucl. Eng. Dept.

1 University of Toledo
Toldeo, Ohio

J. J. Turin

3 University of Washington
Seattle, Washington

A. L. Babb, Dept. of Nucl. Eng.
D. G. Fischbach
K. L. Garlid

1 University of Wisconsin
Madison 6, Wisconsin

M. W. Carbon, Nucl. Eng. Com.

1 Virginia Polytechnic Institute
Blacksburg, Virginia

A. Robeson, Physics Dept.

1 Washington State University
Pullman, Washington

J. P. Spielman, Col. of Eng.

10 Westinghouse Electric Corporation

C. A. Anderson
R. J. French
W. D. Leggett
R. S. Miller
P. M. Murray
R. E. Olsen
W. L. Orr
J. Haley
J. R. Worden
J. H. Wright

No. of Copies

1 Whiteshell Nuclear Research Establishment
Atomic Energy of Canada, Ltd.
Pinawa, Manitoba, Canada

R. B. Lyon, Head-Assessment & Applied Math. Section

ONSITE-HANFORD

1 AEC Chicago Patent Group

R. M. Poteat

1 AEC Richland Operations Office

M. R. Schneller

6 Atlantic Richfield Hanford Company

R. D. Carter
R. E. Isaacson
G. R. Kiel
A. E. Smith
R. E. Tomlinson
ARHCO File

2 Computer Sciences Corporation

E. Z. Block
R. J. Shields

1 Donald W. Douglas Laboratories

J. Greenborg

11 Douglas United Nuclear

P. A. Carlson
C. D. Harrington
H. R. Kosmata
C. W. Kuhlman
W. M. Mathis
R. H. Meichle
E. W. Peacock
R. K. Robinson
DUN File (3)

6 RDT Assistant Director for Pacific Northwest Programs

W. E. Fry
P. G. Holsted (2)
J. B. Kitchen
D. W. Mazur
T. A. Nemzek

No. of Copies

22 WADCO

G. F. Bailey
R. A. Bennett
E. T. Boulette
W. L. Bunch
J. J. Cadwell
J. A. Christensen
E. A. Evans
R. E. Heineman
P. L. Hofmann
R. L. Junkins
W. W. Little
R. E. Peterson
C. A. Rogers
R. E. Schenter
W. F. Sheeley
R. C. Smith
K. L. Young
WADCO Document Control (5)

88 Battelle-Northwest

F. W. Albaugh
C. A. Bennett
S. R. Bierman
C. L. Brown
S. H. Bush
J. L. Carter
N. E. Carter
T. D. Chikalla
D. E. Christensen
R. G. Clark
E. D. Clayton
G. M. Dalen
L. C. Davenport
T. F. Demmitt
D. E. Deonigi
R. L. Dillon
J. R. Divine
B. H. Duane
G. W. R. Endres
P. L. Farnsworth
L. G. Faust
L. G. Federico
J. W. Finnigan
J. C. Fox
M. D. Freshley
J. J. Fuquay
A. G. Gibbs
S. Goldsmith
R. J. Hall
L. E. Hansen
O. K. Harling
C. M. Heeb
H. L. Henry
R. J. Hoch
U. P. Jenquin
B. M. Johnson
G. J. Konzek
D. A. Kottwitz
C. R. Lagergren
D. C. Lehfeldt
B. R. Leonard, Jr.
D. L. Lessor
R. C. Liikala
C. W. Lindenmeier
E. P. Lippincott
R. C. Lloyd
T. I. McSweeney
J. N. Morgan
D. F. Newman
R. E. Nightingale
D. R. Oden, Jr.
L. T. Pederson
R. S. Paul
W. W. Porath
D. L. Prezbindowski
R. H. Purcell
W. L. Purcell
W. A. Reardon
W. D. Richmond
W. C. Roesch
J. T. Russell
L. C. Schmid (10)
G. D. Seybold
R. I. Smith
K. B. Stewart
H. J. Svoboda, Jr.
D. H. Thomsen
G. L. Tingey
V. O. Uotinen
L. D. Williams
N. G. Wittenbrock
W. C. Wolkenhauer
M. G. Zimmerman
Technical Publications (1)
Technical Information (5)